

Highly deformed modes in the *ab initio* symplectic no-core shell model

T Dytrych¹, K D Sviratcheva¹, C Bahri¹, J P Draayer¹ and J P Vary²

¹ Department of Physics and Astronomy, Louisiana State University, Baton Rouge, LA 70803, USA

² Department of Physics and Astronomy, Iowa State University, Ames, IA 50011, USA

Received 9 May 2008

Published 25 July 2008

Online at stacks.iop.org/JPhysG/35/095101

Abstract

We show that highly deformed modes essential for nuclear dynamics modeling can readily be included in the symplectic no-core shell model (Sp-NCSM) space. In particular, a prescription for constructing general deformed k -particle- k -hole (kp - kh) translationally invariant symplectic $\text{Sp}(3, \mathbb{R})$ starting state configurations and symplectic excitations thereof in a fermion-based spherical harmonic oscillator basis is presented. This prescription is used to build the symplectic excitations over all possible $2\hbar\Omega$ $2p$ - $2h$ as well as the most deformed $4\hbar\Omega$ $4p$ - $4h$ $\text{Sp}(3, \mathbb{R})$ configurations in ^{12}C and ^{16}O . The extent to which these configurations enter into low-lying states for these nuclei calculated within the framework of the no-core shell model with a realistic microscopic interaction is then determined. Typically, the addition of these $2p$ - $2h$ and $4p$ - $4h$ representations to the leading $0p$ - $0h$ results grow the overall overlap with the no-core-shell-model eigenstates by 5–10% for a total of 85–90%. And most importantly, even with the addition of these higher-order particle-hole configurations, the dimensionality of the symplectic subspace constitutes a very small fraction of the conventional full no-core shell model space, which reaffirms the relevance of the Sp-NCSM scheme.

1. Introduction

With remarkable progress made in recent years in the development of realistic two- and three-nucleon interactions (e.g., [1–4]), *ab initio* approaches such as the no-core shell model (NCSM) [5], Green's function Monte Carlo methods [6] and coupled cluster expansions [7] have successfully described properties of light nuclei while establishing a link between few-nucleon interactions and many-body nuclear dynamics. However, certain low-lying states, such as the first excited 0^+ state in ^{12}C (with impact on stellar evolution and nucleosynthesis) and excited 0^+ states in ^{16}O continue to remain a challenge for *ab initio* techniques [5, 7, 8]. The presence of highly deformed modes among low-lying states in these nuclei was recognized

early on [9] and attributed to the existence of low-lying, strongly favored 4-particle–4-hole (4p–4h) configurations [10, 11]. These configurations have also been described in terms of an α -cluster dynamics [12]. Typically, α -cluster models do not include other important features, such as spin–orbit splitting effects, nor do they reproduce enhanced electromagnetic transition rates. However, the ability of these models to reproduce cluster-like configurations has made an examination of the microscopic underpinning of α -clustering [13–15]) and α -cluster condensation (see, e.g., [16, 17]) the focus of considerable attention in recent years. In particular, some recent work has advanced the α -cluster concept as a unified framework that includes a model with mixed basis of symplectic $\text{Sp}(3, \mathbb{R})$ and α -cluster configurations that can achieve improved electromagnetic transition rates [18], as well as mean-field molecular dynamics [19, 20] that introduces sub-cluster degrees of freedom. Alternatively, further progress in shell-model calculations has been achieved with model spaces reaching 4p–4h configurations [21–24].

With the goal of providing a microscopic description of phenomena ranging from single-particle effects to clustering correlations and collective rotations, we explore the symplectic $\text{Sp}(3, \mathbb{R})$ symmetry and its role toward advancing the *ab initio* NCSM. The NCSM has been applied to various nuclei from the deuteron through ^{16}O with no limitations on the nature of the realistic two- and three-nucleon interaction [5]. In addition, the Sp-NCSM symplectic extension holds promise to expand the current NCSM space limits by adding significant multi-particle–multi-hole modes of reduced dimensions for equivalent ultra-large NCSM spaces and hence to improve energy convergence. This follows from our recent finding that the physically relevant symplectic $\text{Sp}(3, \mathbb{R})$ basis yields a dramatic reduction of the NCSM space [25, 26]. Specifically, we reported the preponderance of only a few 0p–0h $\text{Sp}(3, \mathbb{R})$ irreducible representations (irreps) within NCSM eigenstates for low-lying states in ^{12}C and ^{16}O [26]. Note that a $N\hbar\Omega$ kp–kh symplectic irrep is classified according to its $N\hbar\Omega$ kp–kh starting state configuration (symplectic bandhead) and, e.g., a $(0\hbar\Omega)$ 0p–0h $\text{Sp}(3, \mathbb{R})$ irrep includes 0p–0h nuclear configurations of the bandhead together with single- and multi-particle excitations built upon these configurations, as described in section 2 (see figure 1 in [27]).

In this paper we show that the symplectic model subspace of the Sp-NCSM can be expanded to include highly deformed modes of physical significance, while maintaining a computationally manageable model space. For example, such configurations include $2\hbar\Omega$ 2p–2h and $4\hbar\Omega$ 4p–4h $\text{Sp}(3, \mathbb{R})$ starting state configurations together with their symplectic excitations (e.g. multiples of $2\hbar\Omega$ 1p–1h and 2p–2h above the starting state). The construction of these configurations in a fermion-based spherical harmonic oscillator (HO) basis (*m*-scheme) is presented in this paper together with a useful prescription for eliminating the spurious center-of-mass motion from the symplectic bandheads, which is vital for the implementation of the translationally invariant Sp-NCSM scheme. The outcome of the present study reveals the role of the $2\hbar\Omega$ 2p–2h and $4\hbar\Omega$ 4p–4h symplectic irreps within the ground-state rotational band in ^{12}C as well as the ^{16}O ground 0^+ state that are reasonably well converged within the framework of the NCSM with the JISP16 realistic interaction [1]. Furthermore, the NCSM eigenstates are examined, for the first time, for their collective properties. This analysis provides insight into the physics and shape deformation of the nuclear systems.

The ability of the Sp-NCSM to accommodate $N\hbar\Omega$ kp–kh $\text{Sp}(3, \mathbb{R})$ irreps is essential for describing states with a pronounced α -cluster structure. Indeed, comparisons of $\text{Sp}(3, \mathbb{R})$ symplectic and α -cluster wavefunctions [18, 28] indicate that these states display a high degree of overlap. In particular, while this holds for 0p–0h symplectic irreps particularly for low oscillator quanta excitations and when built on a strongly deformed intrinsic bandhead, the restriction of the symplectic model subspace to dominant 0p–0h irreps is not sufficient. Recently, mean-field calculations for low-lying 0^+ states in ^{16}O [29] confirm the significant

role of symplectic irreps built over the most deformed $2\hbar\Omega$ 2p–2h and $4\hbar\Omega$ 4p–4h $\text{Sp}(3, \mathbb{R})$ bandheads. In short, while the Sp-NCSM approach can be used to reproduce observed $B(E2)$ values without the need for an effective charge, it can also accommodate highly deformed spatial configurations that include a realization of cluster-like structures [18, 28].

This paper is organized as follows. In section 2, we introduce a prescription for the expansion of an arbitrary translationally invariant $\text{Sp}(3, \mathbb{R})$ irrep built on a $N\hbar\Omega$ kp–kh starting state configuration in an A -nucleon m -scheme basis. In section 3, we examine the role of the $2\hbar\Omega$ 2p–2h and $4\hbar\Omega$ 4p–4h symplectic irreps for low-lying states in ^{12}C and ^{16}O as determined within the framework of the NCSM with the JISP16 realistic interaction [1]. Note that the results are based on the projection of the realistic eigenstates onto the $0p$ – $0h$, $2\hbar\Omega$ 2p–2h and $4\hbar\Omega$ 4p–4h $\text{Sp}(3, \mathbb{R})$ -symmetric basis states and hence are influenced by the NCSM calculations within that limited model space.

2. Construction of translationally invariant symplectic basis states

For A nucleons the 21 distinct bilinear products of the particle momentum ($p_{s\alpha}$) and coordinate ($x_{s\beta}$) operators, $T_{\alpha\beta} = \sum_s p_{s\alpha} p_{s\beta}$, $L_{\alpha\beta} = \sum_s (x_{s\alpha} p_{s\beta} - x_{s\beta} p_{s\alpha})$, $S_{\alpha\beta} = \sum_s (x_{s\alpha} p_{s\beta} + p_{s\alpha} x_{s\beta})$ and $Q_{\alpha\beta} = \sum_s x_{s\alpha} x_{s\beta}$ with $\alpha, \beta = 1, 2, 3$ for the three spatial directions and $s = 1, \dots, A$ yield a realization of the symplectic $\mathfrak{sp}(3, \mathbb{R})$ algebra [27, 30]. It follows from this that the elements of the $\mathfrak{sp}(3, \mathbb{R}) \supset \mathfrak{su}(3) \supset \mathfrak{so}(3)$ algebraic structure include important observables such as the many-particle kinetic energy $\sum_{s,\alpha} p_{s\alpha}^2/2m$, the mass quadrupole moment $Q_{\alpha\beta}$ and angular momentum $L_{\alpha\beta}$ operators, together with multi-shell vibrations and vorticity degrees of freedom for a description of rotational dynamics in a continuous range from irrotational to rigid rotor flows.

Alternatively, the elements of the $\mathfrak{sp}(3, \mathbb{R})$ algebra can linearly be transformed and represented as bilinear products in harmonic oscillator (HO) raising ($b_\alpha^\dagger = \sqrt{\frac{m\Omega}{2\hbar}} x_\alpha - i\sqrt{\frac{1}{2m\hbar\Omega}} p_\alpha$) and lowering ($b_\alpha = (b_\alpha^\dagger)^\dagger$) operators. In this realization, the natural set of the symplectic generators includes the HO Hamiltonian H_0 , which counts the total number of oscillator bosons, together with the eight traceless single-shell $\text{SU}(3)$ generators $C_{\alpha\beta} \sim \sum_s b_{s\alpha}^\dagger b_{s\beta}$, $s = 1, \dots, A$, as well as the six symplectic raising operators $A_{\alpha\beta} = \sum_s b_{s\alpha}^\dagger b_{s\beta}^\dagger$, which raise one particle by two shells (induce a symplectic excitation), and their adjoints, the symplectic lowering operators $B_{\alpha\beta} = \sum_s b_{s\alpha} b_{s\beta}$.

The symplectic generators as described above are not translationally invariant and hence introduce center-of-mass spuriousity in the description of a nuclear system. One way to overcome this problem is to construct the $\text{Sp}(3, \mathbb{R})$ generators in terms of intrinsic coordinates, namely, $x'_{s\alpha} = x_{s\alpha} - X_\alpha$ and $p'_{s\alpha} = p_{s\alpha} - P_\alpha$, defined with respect to the center-of-mass momentum $P_\alpha = \sum_s p_{s\alpha}$ and position $X_\alpha = \frac{1}{A} \sum_s x_{s\alpha}$ [31]. The translationally invariant (intrinsic) $\text{Sp}(3, \mathbb{R})$ generators can then be written in a $\text{SU}(3)$ -coupled form as

$$\begin{aligned}
 A_{\mathcal{E}M}^{(20)} &= \frac{1}{\sqrt{2}} \sum_i [b_i^\dagger \times b_i^\dagger]_{\mathcal{E}M}^{(20)} - \frac{1}{\sqrt{2}A} \sum_{s,t} [b_s^\dagger \times b_t^\dagger]_{\mathcal{E}M}^{(20)} \\
 B_{\mathcal{E}M}^{(02)} &= \frac{1}{\sqrt{2}} \sum_i [b_i \times b_i]_{\mathcal{E}M}^{(02)} - \frac{1}{\sqrt{2}A} \sum_{s,t} [b_s \times b_t]_{\mathcal{E}M}^{(02)} \\
 C_{\mathcal{E}M}^{(11)} &= \sqrt{2} \sum_i [b_i^\dagger \times b_i]_{\mathcal{E}M}^{(11)} - \frac{\sqrt{2}}{A} \sum_{s,t} [b_s^\dagger \times b_t]_{\mathcal{E}M}^{(11)},
 \end{aligned} \tag{1}$$

together with $H_0^{(00)} = \sqrt{3} \sum_i [b_i^\dagger \times b_i]^{(00)} + \frac{3}{2}(A-1)$, where the sums are over all A particles of the system. Clearly, the intrinsic $\text{Sp}(3, \mathbb{R})$ generators (1) can be obtained from the translationally noninvariant $\text{Sp}(3, \mathbb{R})$ generators (the first term for each operator in (1)) after the subtraction of the c.m. two-body operators (last terms in (1)), $A_{\mathcal{L}M}^{(20)\text{cm}} = \frac{1}{\sqrt{2}}[\mathfrak{B}^\dagger \times \mathfrak{B}^\dagger]_{\mathcal{L}M}^{(20)}$, $B_{\mathcal{L}M}^{(02)\text{cm}} = \frac{1}{\sqrt{2}}[\mathfrak{B} \times \mathfrak{B}]_{\mathcal{L}M}^{(02)}$ and $C_{\mathcal{L}M}^{(11)\text{cm}} = \sqrt{2}[\mathfrak{B}^\dagger \times \mathfrak{B}]_{\mathcal{L}M}^{(11)}$. These c.m. operators together with the c.m. excitation number operator,

$$\hat{N}^{\text{cm}} = \mathfrak{B}^\dagger \cdot \mathfrak{B}, \quad (2)$$

are expressed by means of the c.m. harmonic oscillator ladder operators,

$$\mathfrak{B}_\alpha^\dagger = \sqrt{\frac{Am\Omega}{2\hbar}} \left(X_\alpha - \frac{i}{Am\Omega} P_\alpha \right) = \frac{1}{\sqrt{A}} \sum_{i=1}^A b_{i\alpha}^\dagger = (\mathfrak{B}_\alpha)^\dagger, \quad (3)$$

which obey the standard boson commutation relations $[\mathfrak{B}_\alpha, \mathfrak{B}_\beta^\dagger] = \delta_{\alpha\beta}$ and $[\mathfrak{B}_\alpha^\dagger, \mathfrak{B}_\beta^\dagger] = 0$. Hence, the c.m. operators generate the $\text{Sp}(3, \mathbb{R})$ group with representations equivalent to the $\text{Sp}(3, \mathbb{R})$ representation of a single-particle space, namely $(k0)$ for a $k\hbar\Omega$ c.m. excitation. In addition, the c.m. symplectic generators commute with the intrinsic $\text{Sp}(3, \mathbb{R})$ operators (1).

The symplectic basis states (labeled in standard notation [27, 30]) are constructed by acting with polynomials \mathcal{P} in the symplectic raising operator, $A^{(20)}$ (1), on a set of basis states of the symplectic bandhead, $|\sigma\rangle$, which is a $\text{Sp}(3, \mathbb{R})$ lowest-weight state,

$$|\sigma n \rho \omega \kappa (LS) J M_J\rangle = [\mathcal{P}^n (A^{(20)}) \times |\sigma\rangle]_{\kappa(LS) J M_J}^{\rho \omega}, \quad (4)$$

where $\sigma \equiv N_\sigma(\lambda_\sigma \mu_\sigma)$ labels $\text{Sp}(3, \mathbb{R})$ irreps, $n \equiv N_n(\lambda_n \mu_n)$ and $\omega \equiv N_\omega(\lambda_\omega \mu_\omega)$. The quantum number $N_\omega = N_\sigma + N_n$ is the total number of oscillator quanta related to the eigenvalue, $N_\omega \hbar \Omega$, of a HO Hamiltonian that is free of spurious modes. The $(\lambda_n \mu_n)$ set gives the overall $\text{SU}(3)$ symmetry of $\frac{N_n}{2}$ coupled raising operators in \mathcal{P} and $(\lambda_\omega \mu_\omega)$ specifies the $\text{SU}(3)$ symmetry of the symplectic state. In accordance with the mapping [32] between the shell-model $(\lambda \mu) \text{SU}(3)$ labels and the shape variables of the Bohr–Mottelson collective model [33], namely, the prolate elongation $\beta > 0$ and the $0 \leq \gamma \leq \pi/2$ asymmetry parameter, the symplectic basis states bring forward important information about the nuclear shapes and deformation in terms of their $(\lambda_\omega \mu_\omega) \text{SU}(3)$ symmetry (4). For example, $(\lambda_\omega 0)$ and $(0 \mu_\omega)$ describe prolate ($\gamma \sim 0^\circ$) and oblate ($\gamma \sim 60^\circ$) shapes, respectively, with increasing λ_ω (μ_ω) toward larger deformations, β .

The symplectic basis states, which are generated by the translationally invariant form of the $A^{(20)}$ symplectic raising operators (1), are free of c.m. spurious excitations provided that the $|\sigma\rangle$ symplectic bandhead is also non-spurious. The basis states, $|\sigma \kappa_0 (L_0 S_0) J_0 M_0\rangle$, of the symplectic bandhead are the starting state configurations upon which a $\text{Sp}(3, \mathbb{R})$ irrep is built according to (4). Consequently, these states are annihilated upon the action of the $B_{\mathcal{L}M}^{(02)}$ symplectic lowering operators,

$$B_{\mathcal{L}M}^{(02)} |\sigma \kappa_0 (L_0 S_0) J_0 M_0\rangle = 0. \quad (5)$$

By construction, the symplectic bandhead, and hence the basis states of the corresponding $\text{Sp}(3, \mathbb{R})$ irrep (4), can be expanded in a m -scheme basis. This is the same basis used in the NCSM, and thus it facilitates calculations and symmetry identification. In our study, the symplectic bandheads are constructed in a proton–neutron formalism as $\text{SU}(3)_{(\lambda_\sigma \mu_\sigma)} \times \text{SU}(2)_{S_0}$ -symmetric linear combinations of m -scheme configurations of a given N_σ . In the case of 0p–0h symplectic bandheads, the value of N_σ corresponds to the lowest HO energy of a system of A nucleons. The construction formula is given as

$$|(\xi \rho_\sigma) \sigma \kappa_0 (L_0 S_0) J_0 M_0\rangle = [\mathcal{P}_{\mathbf{I}_\pi S_\pi}^{N_\pi(\lambda_\pi \mu_\pi)} (a_\pi^\dagger) \times \mathcal{P}_{\mathbf{I}_\nu S_\nu}^{N_\nu(\lambda_\nu \mu_\nu)} (a_\nu^\dagger)]_{\kappa_0 (L_0 S_0) J_0 M_0}^{\rho_\sigma N_\sigma(\lambda_\sigma \mu_\sigma)} |0\rangle, \quad (6)$$

where $N_\pi + N_\nu = N_\sigma$, ξ schematically denotes the additional quantum numbers included to distinguish between different bandhead constructions for protons and neutrons, $\{\mathbf{f}_\pi N_\pi(\lambda_\pi \mu_\pi) S_\pi, \mathbf{f}_\nu N_\nu(\lambda_\nu \mu_\nu) S_\nu\}$ (with \mathbf{f}_π and \mathbf{f}_ν described below), and ρ_σ gives the multiplicity of σ for a given ξ set of quantum numbers. (Note that $\rho_\sigma = 1$ for 0p–0h $\text{Sp}(3, \mathbb{R})$ states.) In (6), $\mathcal{P}_{\mathbf{f}_\pi S_\pi}^{N_\pi(\lambda_\pi \mu_\pi)}$ and $\mathcal{P}_{\mathbf{f}_\nu S_\nu}^{N_\nu(\lambda_\nu \mu_\nu)}$ are polynomials of proton (a_π^\dagger) and neutron (a_ν^\dagger) creation operators coupled to good $\text{SU}(3) \times \text{SU}(2)$ symmetry, that is to definite $(\lambda \mu)$ and spin S values,

$$\begin{aligned} \mathcal{P}_{\mathbf{f}_\pi S_\pi}^{N_\pi(\lambda_\pi \mu_\pi)} &= \left[a_{\pi \frac{1}{2}}^{\dagger(\eta_1 0)} \times \cdots \times a_{\pi \frac{1}{2}}^{\dagger(\eta_{Z0})} \right]_{S_\pi}^{N_\pi(\lambda_\pi \mu_\pi)}, \\ \mathcal{P}_{\mathbf{f}_\nu S_\nu}^{N_\nu(\lambda_\nu \mu_\nu)} &= \left[a_{\nu \frac{1}{2}}^{\dagger(\eta_1' 0)} \times \cdots \times a_{\nu \frac{1}{2}}^{\dagger(\eta_{N'0})} \right]_{S_\nu}^{N_\nu(\lambda_\nu \mu_\nu)}. \end{aligned} \quad (7)$$

The construction of the $\text{SU}(3) \times \text{SU}(2)$ symmetry-adapted many-fermion states (6) is based on the fact that the fermion creation operators are irreducible $\text{SU}(3) \times \text{SU}(2)$ tensors, i.e. $a_{\eta(l \frac{1}{2}) j m_j}^\dagger \rightarrow a_{(l \frac{1}{2}) j m_j}^{\dagger(\eta 0)}$, with a $\text{SU}(3)$ character of $(\eta 0)$ and spin $\frac{1}{2}$ [34]. Here, the principal quantum number $\eta = 0, 1, 2, \dots$ labels a HO shell and the orbital momentum $l = \eta, \eta - 2, \dots, 0(1)$. The nucleon distribution over HO shells is given by the principal quantum numbers $\mathbf{f}_\pi = \{\eta_1, \dots, \eta_Z\}$ for Z protons and $\mathbf{f}_\nu = \{\eta_1', \dots, \eta_{N'}'\}$ for N neutrons, and uniquely determines the $\text{SU}(3)$ quantum numbers, $(\lambda_\pi \mu_\pi)$ and $(\lambda_\nu \mu_\nu)$, respectively.

The symplectic bandheads generated by the procedure described above (6) are not translationally invariant with the exception of those constructed within the $0\hbar\Omega$ model space [35]. Techniques, based on diagonalization of the c.m. harmonic oscillator Hamiltonian or use of c.m. creation operators (3) to identify and eliminate spurious c.m. excitations in the $\text{SU}(3)$ symmetry-adapted basis, were initially proposed by Verhaar [36] and Hecht [37], respectively. Here we use an alternative and simpler approach based on $\text{U}(3)$ symmetry-preserving c.m. projecting operators. The method was briefly outlined by Hecht [37] but never utilized for eliminating the c.m. spuriousity from the symplectic basis states.

The projection technique is based on the fact that a general $\text{SU}(3)$ symmetry-adapted A -particle state of $n_{\max} \hbar\Omega$ excitations above the lowest energy configuration can be written in a $\text{SU}(3)$ -coupled form as

$$|(\lambda \mu) \alpha\rangle = \sum_{n=0}^{n_{\max}} \sum_{(\lambda \mu)_{\text{intr}}} c_n^{(\lambda \mu)_{\text{intr}}} |(n 0) \otimes (\lambda \mu)_{\text{intr}}; (\lambda \mu) \alpha\rangle, \quad (8)$$

where $\alpha = \{\kappa L M\}$ and $c_n^{(\lambda \mu)_{\text{intr}}}$ denote the coefficients. The $\text{SU}(3)$ quantum numbers, $(\lambda \mu)_{\text{intr}}$, label the intrinsic wavefunctions of $(n_{\max} - n) \hbar\Omega$ excitations that are coupled with the c.m. $\text{SU}(3)$ irreps $(n 0)$ of $n \hbar\Omega$ excitations into the final $\text{SU}(3)$ symmetry $(\lambda \mu)$. Note that for the non-spurious part of the state, $n = 0$, the quantum numbers $(\lambda \mu)_{\text{intr}}$ coincide with $(\lambda \mu)$.

In order to eliminate the c.m. spuriousity from A -particle $\text{SU}(3)$ -symmetric states, such as the symplectic bandheads, one needs to project out all the $n \geq 1$ terms on the right-hand side of the expansion (8) as they describe excited (spurious) c.m. motion. This is done by employing the simplest $\text{U}(3)$ Casimir invariant, namely, the c.m. number operator \hat{N}^{cm} (2), in a $\text{U}(3)$ symmetry-preserving projecting operator,

$$\hat{P}(n_{\max}) = \prod_{k_0=1}^{n_{\max}} \left(1 - \frac{\hat{N}^{\text{cm}}}{k_0} \right). \quad (9)$$

The $|(n 0) \otimes (\lambda \mu)_{\text{intr}}; (\lambda \mu) \alpha\rangle$ states (8) are eigenstates of \hat{N}^{cm} with eigenvalues n . Therefore, they are also eigenstates of the $\hat{P}(n_{\max})$ operator with eigenvalues equal to 0 for excitations $n = 1, \dots, n_{\max}$ and 1 when $n = 0$, which corresponds to a non-spurious state. Therefore, the

c.m. spurious excitations vanish under the action of $\hat{P}(n_{\max})$, while a non-spurious state (or the spurious-free part of a state) remains unaltered. The non-spurious states, which are obtained after the projection, are properly orthonormalized and then utilized in the calculations.

3. Results and discussions

The lowest-lying eigenstates of the deformed ^{12}C nucleus and the ‘closed-shell’ ^{16}O nucleus were calculated using the NCSM as implemented through the many fermion dynamics (MFD) code [38] with an effective interaction derived from the realistic JISP16 NN potential [1] for different $\hbar\Omega$ oscillator strengths and with the bare interaction. We present results for the $J = 0_{\text{gs}}^+$ and the lowest $J = 2^+(\equiv 2_1^+)$ and $J = 4^+(\equiv 4_1^+)$ states in ^{12}C and the 0_{gs}^+ ground state in ^{16}O , which appear to be reasonably well converged in the $N_{\max} = 6$ NCSM basis space. These states were analyzed for their symplectic symmetry structure by projecting the NCSM wavefunctions onto a symplectic model subspace, which in addition to the 0p–0h $\text{Sp}(3, \mathbb{R})$ irreps considered previously [26] now took into account complementary $k\hbar\Omega$ kp–kh symplectic irreps, $k = 2, 4$. This analysis provides further insight into the physics and geometry of a nuclear system since nuclear collective states with well-developed quadrupole and monopole vibrations as well as collective rotations are described naturally in terms of $\text{Sp}(3, \mathbb{R})$ irreps. Indeed, group-theoretical approaches, which exploit the symplectic symmetry, typically achieve quite reasonable microscopic descriptions of the low-lying energy spectrum and $B(E2)$ values in light nuclei (see, e.g., [29, 39–42]).

The prescription described in section 2 was used to construct all translationally invariant $2\hbar\Omega$ 2p–2h $\text{Sp}(3, \mathbb{R})$ bandheads and the most deformed $4\hbar\Omega$ 4p–4h symplectic bandheads in ^{12}C and ^{16}O . The total number of the $2\hbar\Omega$ 2p–2h symplectic bandheads is around 10^3 in the case of ^{12}C , and approximately half of this amount for ^{16}O . However, similarly to the case of 0p–0h symplectic bandheads [26], only a relatively small fraction of the $2\hbar\Omega$ 2p–2h symplectic bandheads project at the nonnegligible level onto the low-lying NCSM wavefunctions.

The projection of the NCSM eigenstates under consideration onto symplectic states shows that for ^{12}C there are 20 important $2\hbar\Omega$ 2p–2h symplectic bandheads in the $N_{\max} = 6$ ($6\hbar\Omega$ model space). The typical dimension of a symplectic irrep in the $N_{\max} = 6$ space is on the order of 10^2 as compared to 10^7 for the full NCSM m -scheme basis space. In addition, the J angular momentum is a good quantum number for the symplectic basis (4) (but not for the m -scheme basis), and hence the symplectic space can be further reduced to only the subspaces specified by the J values under consideration. In the present study, these are $J = 0, 2$ and 4 for ^{12}C and $J = 0$ for ^{16}O . As N_{\max} is increased the dimension of the $J = 0, 2$ and 4 symplectic space built on the 0p–0h $\text{Sp}(3, \mathbb{R})$ irreps grows very slowly compared to the NCSM space dimension [25]. The net result is that as N_{\max} increases the symplectic model subspace is an ever smaller fraction of the NCSM basis space, even when the most dominant $2\hbar\Omega$ 2p–2h $\text{Sp}(3, \mathbb{R})$ irreps are included (table 1). The reduction is even more dramatic in the case of ^{16}O , where only the $J = 0$ subspace is taken into account for the 0^+ states (table 1). This means that the space spanned by the set of relevant symplectic basis states is computationally manageable even when high- $\hbar\Omega$ configurations are included. Of course, if one were to include all possible $N\hbar\Omega$ kp–kh starting state configurations in the ($N \leq N_{\max}$) space, and allowed multiples thereof, one would span the full NCSM model space.

3.1. Ground-state rotational band in ^{12}C

In the case of ^{12}C , the symplectic model space is expanded beyond the 0p–0h subspace to include the most important $2\hbar\Omega$ 2p–2h $\text{Sp}(3, \mathbb{R})$ irreps, those with a nonnegligible overlap

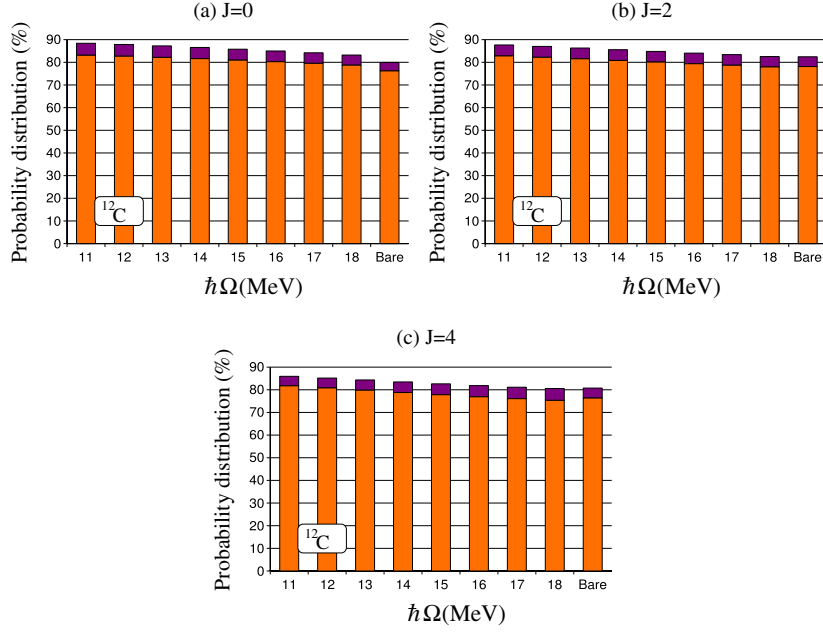


Figure 1. Projection of NCSM wavefunctions for ^{12}C onto the dominant 0p–0h (orange, lower bars) and $2\hbar\Omega$ 2p–2h (purple, upper bars) $\text{Sp}(3, \mathbb{R})$ irreps for: (a) 0_{gs}^+ , (b) 2_1^+ and (c) 4_1^+ as a function of the $\hbar\Omega$ oscillator strength. Results are also shown for the bare interaction at $\hbar\Omega = 15$ MeV (column on the far right of each figure). The maximum scale of the vertical axis is 90%.

Table 1. Space dimension ratios, $R_{0(2)}^{\text{Sp}}$ in %, of the dominant 0p–0h (0p–0h + 2p–2h) $\text{Sp}(3, \mathbb{R})$ irreps with $J = 0, 2$ and 4 for ^{12}C , and $J = 0$ for ^{16}O with respect to the NCSM space size, D^{NCSM} , as a function of maximum allowed $\hbar\Omega$ excitations, N_{max} .

$N_{\text{max}}\hbar\Omega$	$0\hbar\Omega$	$2\hbar\Omega$	$4\hbar\Omega$	$6\hbar\Omega$	$8\hbar\Omega$	$10\hbar\Omega$	$12\hbar\Omega$
^{12}C							
R_0^{Sp} (%)	25.5	0.38	0.019	1.6×10^{-3}	1.7×10^{-4}	2.3×10^{-5}	3.7×10^{-6}
R_2^{Sp} (%)	25.5	1.29	0.087	8.5×10^{-3}	1.0×10^{-3}	1.3×10^{-4}	1.6×10^{-5}
D^{NCSM}	51	1.8×10^4	1.1×10^6	3.3×10^7	5.9×10^8	7.8×10^9	8.0×10^{10}
^{16}O							
R_0^{Sp} (%)	100	0.16	0.001	2.6×10^{-5}	1.1×10^{-6}	6.7×10^{-8}	5.7×10^{-9}
R_2^{Sp} (%)	100	0.88	0.012	4.5×10^{-4}	2.6×10^{-5}	2.1×10^{-6}	2.1×10^{-8}
D^{NCSM}	1	1.2×10^3	3.4×10^5	2.6×10^7	9.7×10^8	2.2×10^{10}	3.8×10^{11}

to the NCSM eigenstates for the $J = 0, 2$ and 4 states in the ground-state rotational band. The symplectic space expansion improves the overlaps between these NCSM eigenstates and the $\text{Sp}(3, \mathbb{R})$ -symmetric basis by about 5% (figure 1). (Note that for these states $4\hbar\Omega$ 4p–4h symplectic irreps are found to be negligible.) Overall, approximately 85% of the NCSM eigenstates fall within a subspace spanned by the most significant 3 0p–0h and 20 $2\hbar\Omega$ 2p–2h $\text{Sp}(3, \mathbb{R})$ irreps. As one varies the $\hbar\Omega$ oscillator strength, the projection changes slightly reaching close to 90% for $\hbar\Omega = 11$ MeV.

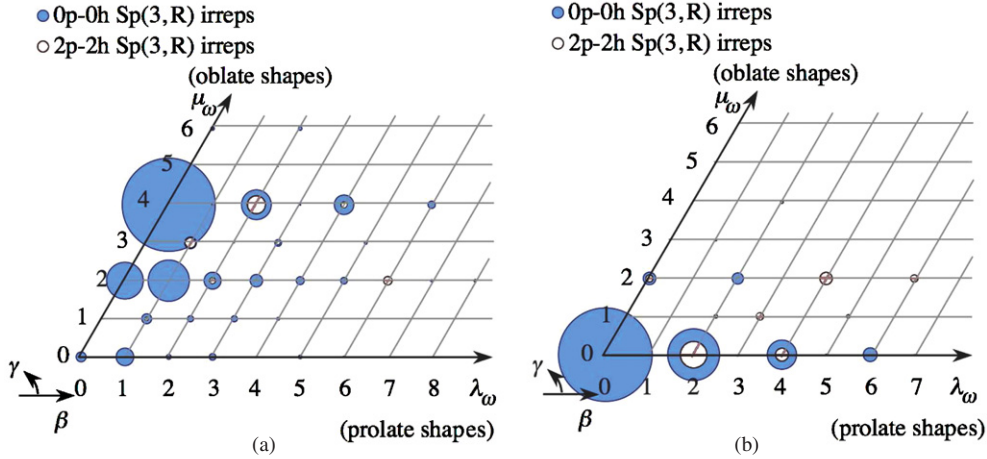


Figure 2. Probabilities (specified by the area of the circles) for the symplectic states which make up the most important 0p–0h (blue circles) and $2\hbar\Omega$ 2p–2h (empty circles) symplectic irreps, within the 0^+ ground state in (a) ^{12}C and (b) ^{16}O , calculated by NCSM, $\hbar\Omega = 15$ MeV. The $\text{Sp}(3, \mathbb{R})$ states are grouped according to their $(\lambda_\omega \mu_\omega)\text{SU}(3)$ symmetry, which is mapped onto the $(\beta\gamma)$ shape variables of the collective model (see the text for further details).

As expected for the ^{12}C ground-state rotational band, oblate shapes dominate, especially among the $0\hbar\Omega$ components (figure 2(a)). The significance of the most important $(\lambda_\sigma \mu_\sigma) = (24)$ and $(13)2\hbar\Omega$ 2p–2h symplectic irreps, in addition to the 0p–0h $\text{Sp}(3, \mathbb{R})$ irrep contribution, clearly indicates a propensity of the $2\hbar\Omega$ components in the NCSM ground-state band toward oblate deformed shapes. However, it is interesting to note that the most prolate deformed configuration is also present as indicated by a non-zero projection onto the (62) symplectic bandhead. The symplectic excitations above the relevant $\text{Sp}(3, \mathbb{R})$ bandheads point to the development of a more complex shape structure as seen, for example, in figure 2 for the ^{12}C ground state. Among these, the stretched symplectic states appear to be of a special interest as they usually possess larger overlaps with the realistic states under consideration as compared to the other symplectic excitations. The stretched states are those with $\mu_\omega = \mu_\sigma$ and maximum value of λ_ω , namely $\lambda_\sigma + N_n$ for $N_n\hbar\Omega$ excitations above the $(\lambda_\sigma \mu_\sigma)$ symplectic bandhead. These correspond to horizontal (same μ_ω) increments of two λ_ω units in the plane of figure 2 starting from the bandhead configuration. Note that, as shown in [25], the symplectic structure (dominant $\text{Sp}(3, \mathbb{R})$ irreps) and hence the geometry of *converged* NCSM eigenstates is almost independent of whether the bare or renormalized interaction is used. While very small contributions of additional $N\hbar\Omega$ kp–kh $\text{Sp}(3, \mathbb{R})$ irreps may be observed with increasing model space size, the results presented in figure 2 are expected to remain almost the same reflecting the true collective nature of the states under consideration.

The dominance of the highly deformed symplectic states within the most important $2\hbar\Omega$ 2p–2h $\text{Sp}(3, \mathbb{R})$ irreps also enhances the corresponding $B(E2 : 2_1^+ \rightarrow 0_{\text{gs}}^+)$ values, which have been calculated for ^{12}C within a 0p–0h symplectic irrep model space [26]. The $B(E2 : 2_1^+ \rightarrow 0_{\text{gs}}^+)$ estimates are found to closely reproduce the experiment for $\hbar\Omega = 11$ MeV but to get smaller with increasing $\hbar\Omega$ oscillator strength [26].

3.2. Ground state in ^{16}O

A much more interesting scenario is observed for the low-lying 0^+ states in ^{16}O . Here, the projection of the NCSM eigenstates onto the symplectic subspace can also be compared to

Table 2. Projection of the ground 0_{gs}^+ and first excited (not fully converged) 0_2^+ NCSM states in ^{16}O onto the dominant $2\hbar\Omega$ 2p–2h symplectic bandheads, $\hbar\Omega = 12$ MeV.

	Number of bandheads	Symplectic bandhead		Probability (%)
		$(\lambda_\sigma \mu_\sigma)$	spin S	
$J = 0_{\text{gs}}^+$	5	(2 0)	0	2.75
	3	(4 2)	0	0.62
	2	(2 0)	2	0.60
	1	(4 2)	2	0.33
$J = 0_2^+$	3	(4 2)	0	29.17
	5	(2 0)	0	3.37
	2	(5 0)	1	1.18
	7	(3 1)	1	0.96

results obtained in the framework of the simple $\alpha+^{12}\text{C}$ cluster model [18, 28]. The latter describes ^{16}O as being made up of α and ^{12}C fragments frozen to the lowest shell-model states with their relative motion carrying arbitrary excitations. The overlaps between the symplectic states and the $\alpha+^{12}\text{C}$ cluster model wavefunctions have been evaluated analytically [18, 28] and it was found that particular symplectic states overlap at a significant level with the corresponding cluster model wavefunctions. This can yield insight into the α -cluster structure of the low-lying 0^+ NCSM eigenstates in ^{16}O .

The $0\text{p}–0\text{h}$ symplectic model subspace analysis for the ^{16}O ground state [26] reveals the dominance of the $(00)S = 0$ symplectic irrep, which is 80 – 75% of the NCSM realistic wavefunction for values of the oscillator strength $\hbar\Omega = 12$ MeV to 16 MeV [26]. The $0\hbar\Omega$ projection of the $(00)S = 0\text{Sp}(3, \mathbb{R})$ irrep, around 40 – 55% for the same $\hbar\Omega$ range, reflects the spherical shape preponderance in the ground state of ^{16}O (figure 2(b)). In addition, a relatively significant mixture of slightly prolate deformed shapes is observed and they are predominantly associated with stretched symplectic excitation states (along the horizontal λ_ω axis in figure 2(b)). Among them, the most significant mode with a projection onto the NCSM state of $\sim 13\%$ (for $\hbar\Omega = 16$ MeV) up to $\sim 25\%$ (for $\hbar\Omega = 12$ MeV) is described by the $2\hbar\Omega$ (20) 1p–1h and weaker 2p–2h $\text{Sp}(3, \mathbb{R})$ -symmetric excitations built over the $(00)S = 0$ 0p–0h symplectic bandhead. This $2\hbar\Omega$ (20) symplectic configuration projects at the 65% level [28] on the corresponding $\alpha+^{12}\text{C}$ cluster model wavefunction. Orthogonal to these excitations, the $(20)S = 0$ 2p–2h symplectic bandhead constructed at the $2\hbar\Omega$ level is found to be the most dominant among the $2\hbar\Omega$ 2p–2h $\text{Sp}(3, \mathbb{R})$ bandheads when compared to the NCSM eigenstates (table 2, figure 2(b)). This means that the appearance of the $2\hbar\Omega$ 2p–2h $\text{Sp}(3, \mathbb{R})$ bandheads in the ground state of ^{16}O is governed in such a way to preserve the shape coherence of all the significant $2\hbar\Omega$ configurations. In addition, the contribution of the most deformed $4\hbar\Omega$ 4p–4h $\text{Sp}(3, \mathbb{R})$ irrep to the ^{16}O ground state is found to be very small, $\sim 10^{-4}\%$.

As compared to the outcome of the $0\text{p}–0\text{h}$ analysis, the inclusion of the $2\hbar\Omega$ 2p–2h $\text{Sp}(3, \mathbb{R})$ irreps constructed over the most significant symplectic bandheads improves the overlaps of the selected symplectic basis with the NCSM eigenstate for the ^{16}O ground state by about 10%. As a result, the ground state in ^{16}O as calculated by NCSM projects at the 85–90% level onto the $J = 0$ symplectic symmetry-adapted basis (figure 3(a)) with a total dimensionality of only $\approx 0.001\%$ of the NCSM space.

Illustrative examples, where the inclusion of highly deformed modes is essential for *ab initio* shell model calculations, are the second 0_2^+ and third 0_3^+ states in ^{16}O . It is important

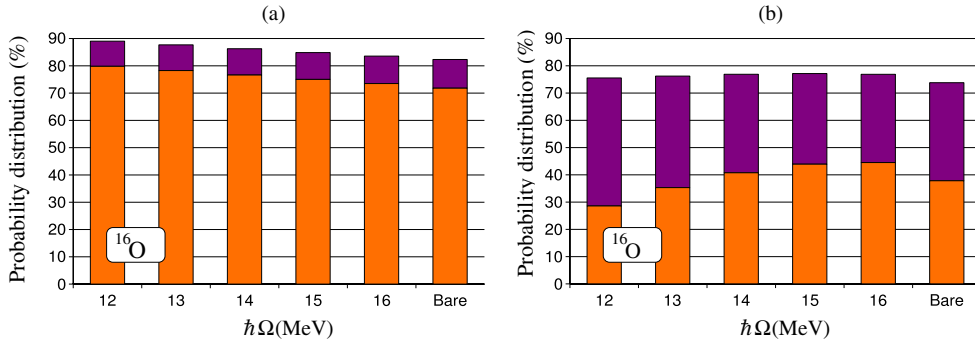


Figure 3. Projection of (a) the ground state 0_{gs}^+ and (b) the first excited (not fully converged) 0_2^+ NCSM states for ^{16}O as a function of the $\hbar\Omega$ oscillator strength onto the 0p–0h (orange, lower bars) $\text{Sp}(3, \mathbb{R})$ irrep and the dominant $2\hbar\Omega$ 2p–2h (purple, upper bars) $\text{Sp}(3, \mathbb{R})$ irreps. Results are also shown for the bare interaction at $\hbar\Omega = 15$ MeV (column on the far right of each figure). The maximum scale of the vertical axis is 90%.

to note that the corresponding NCSM states are not fully converged and the $6\hbar\Omega$ model space is quite restrictive for the development of strong 4p–4h correlations. However, the importance of the $2\hbar\Omega$ 2p–2h $\text{Sp}(3, \mathbb{R})$ irreps (e.g., see (figure 3(b))) and the cluster structure within the second-lying 0^+ NCSM eigenstate has already started to emerge in the $6\hbar\Omega$ model space. Namely, the most deformed $2\hbar\Omega$ 2p–2h $\text{Sp}(3, \mathbb{R})$ irrep (42), which dominates the NCSM 0_2^+ state at the current level of convergence (table 2), projects at the 100% level onto the corresponding $(42)\alpha+^{12}\text{C}$ cluster model wavefunction [28]. This is in addition to the significant overlap between the cluster states [28] and the $2\hbar\Omega$ (20) configurations, which dominate the 0p–0h $\text{Sp}(3, \mathbb{R})$ contribution to the 0_2^+ NCSM state (figure 3(b) (orange, lower bars)). The results suggest the need for exploring the Sp-NCSM scheme with model spaces beyond $N_{\max} = 6$ to achieve convergence of such highly deformed collective modes.

4. Conclusion

This study presents a prescription to include important, highly deformed multi-particle–multi-hole configurations in the Sp-NCSM basis space for *ab initio* descriptions of low-lying states in light atomic nuclei. We focus on the lowest 0_{gs}^+ , 2_1^+ and 4_1^+ states in ^{12}C and the ^{16}O ground state that are reasonably well converged in the $6\hbar\Omega$ -NCSM with the JISP16 realistic interaction. These states are found to project at the 85–90% level onto a very few 0p–0h and $2\hbar\Omega$ 2p–2h spurious center-of-mass free symplectic irreps. The addition of these $2\hbar\Omega$ 2p–2h symplectic irreps (associated with $2\hbar\Omega$ 2p–2h configurations and symplectic particle–hole excitations thereof up through the $6\hbar\Omega$ model space) to the 0p–0h $\text{Sp}(3, \mathbb{R})$ irrep space improves the overlaps by about 5% (for ^{12}C) and 10% (for ^{16}O), while the total dimensionality of the symplectic basis remains only a fraction ($\approx 10^{-3}\%$) that of the NCSM space.

The analysis of the results shows that the converged NCSM low-lying states can be described with only a few 0p–0h and $2\hbar\Omega$ 2p–2h $\text{Sp}(3, \mathbb{R})$ irreps and typically the corresponding symplectic bandheads are the most deformed ones. In addition, we found that the most significant symplectic states built over these $\text{Sp}(3, \mathbb{R})$ bandheads tend to be the most deformed (stretched $\text{SU}(3)$ coupling) configurations.

While the most deformed $4\hbar\Omega$ 4p–4h symplectic irreps do not play a significant role in the converged NCSM eigenstates under consideration, they are vital toward microscopic

description of low-lying highly deformed modes, which imply the necessity of employing model spaces beyond what can be achieved under the NCSM current computational limits. As we show that these modes can be accommodated within the general framework of the $\text{Sp}(3, \mathbb{R})$ model with $0p-0h$, $2\hbar\Omega$ $2p-2h$, $4\hbar\Omega$ $4p-4h$, and maybe higher $N\hbar\Omega$ $kp-kh$ starting state configurations, the Sp-NCSM scheme is expected to model cluster-like phenomena and to reproduce observed $B(E2)$ values by extending the NCSM model space only along the relevant symplectic states of a comparatively small dimensionality up through high $\hbar\Omega$ configurations (high N_{\max}).

Acknowledgments

Discussions with many colleagues, but especially Bruce R Barrett, during the initial phases of this project are gratefully acknowledged. This work was supported by the US National Science Foundation, grants 0140300 and 0500291, and the Southeastern Universities Research Association, as well as, in part, by the US Department of Energy Grant DE-FG02-87ER40371. Tomáš Dytrych acknowledges supplemental support from the Graduate School of Louisiana State University.

References

- [1] Shirokov A M, Mazur A I, Zaytsev S A, Vary J P and Weber T A 2004 *Phys. Rev. C* **70** 044005
Shirokov A M, Vary J P, Mazur A I, Zaytsev S A and Weber T A 2005 *Phys. Lett. B* **621** 96
Shirokov A M, Vary J P, Mazur A I and Weber T A 2007 *Phys. Lett. B* **644** 33
- [2] Machleidt R 2001 *Phys. Rev. C* **63** 024001
- [3] Coon S A and Han H K 2001 *Few-Body Syst.* **30** 131
- [4] Entem D R and Machleidt R 2003 *Phys. Rev. C* **68** 041001
- [5] Navrátil P, Vary J P and Barrett B R 2000 *Phys. Rev. Lett.* **84** 5728
Navrátil P, Vary J P and Barrett B R 2000 *Phys. Rev. C* **62** 054311
Navrátil P and Ormand W E 2003 *Phys. Rev. C* **68** 034305
- [6] Pieper S, Varga K and Wiringa R B 2002 *Phys. Rev. C* **66** 044310
Pieper S C 2005 *Nucl. Phys. A* **751** 516c
- [7] Włoch M, Dean D J, Gour J R, Hjorth-Jensen M, Kowalski K, Papenbrock T and Piecuch P 2005 *Phys. Rev. Lett.* **94** 212501
- [8] Vary J P 2005 *Int. J. Mod. Phys. E* **14** 1
- [9] Morinaga H 1956 *Phys. Rev.* **101** 254
- [10] Brown G E and Green A M 1966 *Nucl. Phys.* **75** 401
- [11] Das Gupta S and de Takacsy N 1969 *Phys. Rev. Lett.* **22** 1194
- [12] Ikeda K, Takigawa N and Horiuchi H 1968 *Prog. Theor. Phys. Suppl.* (extra number) 464
Ikeda K *et al* 1980 *Prog. Theor. Phys. Suppl.* **68** 1
- [13] Filikhin I N and Yakovlev S L 2000 *Phys. At. Nucl.* **63** 343
- [14] Fedotov S I, Kartavtsev O I, Kochkin V I and Malykh A V 2004 *Phys. Rev. C* **70** 014006
- [15] Maruhn J A *et al* 2006 *Phys. Rev. C* **74** 044311
- [16] Tohsaki A, Horiuchi H, Schuck P and Röpke G 2001 *Phys. Rev. Lett.* **87** 192501
- [17] Funaki Y, Tohsaki A, Horiuchi H, Schuck P and Röpke G 2003 *Phys. Rev. C* **67** R051306
- [18] Hecht K T 1978 *J. Phys. Soc. Japan* **44** (Suppl.) 232
Hecht K T and Braunschweig D 1978 *Nucl. Phys. A* **295** 34
Suzuki Y and Hecht K T 1986 *Nucl. Phys. A* **455** 315
Suzuki Y and Hara S 1989 *Phys. Rev. C* **39** 658
- [19] Kanada-En'yo Y 1998 *Phys. Rev. Lett.* **81** 5291
Kanada-En'yo Y 2007 *Prog. Theor. Phys.* **117** 655
- [20] Chernykh M, Feldmeier H, Neff T, von Neumann-Cosel P and Richter A 2007 *Phys. Rev. Lett.* **98** 032501
- [21] Zuker A P, Buck B and McGrory J B 1968 *Phys. Rev. Lett.* **21** 39

- [22] Ellis P J and Engeland T 1970 *Nucl. Phys. A* **144** 161
Engeland T and Ellis P J 1972 *Nucl. Phys. A* **181** 368
- [23] Haxton W C and Johnson C 1990 *Phys. Rev. Lett.* **65** 1325
- [24] Warburton E K, Brown B A and Millener D J 1992 *Phys. Lett. B* **293** 7
- [25] Dytrych T, Sviratcheva K D, Bahri C, Draayer J P and Vary J P 2007 *Phys. Rev. Lett.* **98** 162503
- [26] Dytrych T, Sviratcheva K D, Bahri C, Draayer J P and Vary J P 2007 *Phys. Rev. C* **76** 014315
- [27] Rosensteel G and Rowe D J 1977 *Phys. Rev. Lett.* **38** 10
- [28] Suzuki Y 1986 *Nucl. Phys. A* **448** 395
- [29] Rowe D J, Thiamova G and Wood J L 2006 *Phys. Rev. Lett.* **97** 202501
- [30] Rosensteel G and Rowe D J 1980 *Ann. Phys., NY* **126** 343
Rowe D J 1985 *Rep. Prog. Phys.* **48** 1419
- [31] Rosensteel G 1980 *Nucl. Phys. A* **341** 397
- [32] Castanos O, Draayer J P and Leschber Y 1988 *Z. Phys. A* **329** 33
- [33] Bohr A and Mottelson B R 1953 *Mat.-Fys. Medd. K. Dan. Vidensk. Selsk.* **27** 16
- [34] Draayer J P 1973 *Nucl. Phys.* **216** 457
Wybourne B G 1973 *Classical Groups for Physicists* (New York: Wiley)
- [35] Elliott J P and Skyrme T H R 1955 *Proc. R. Soc. A* **232** 561
- [36] Verhaar B J 1960 *Nucl. Phys.* **21** 508
- [37] Hecht K T 1971 *Nucl. Phys. A* **170** 34
- [38] Vary J P 1992 *The Many-Fermion-Dynamics Shell-Model Code* (Iowa City, IO: Iowa State University) (unpublished)
Vary J P and Zheng D C 1994 *The Many-Fermion-Dynamics Shell-Model Code* (Iowa City, IO: Iowa State University) (unpublished).
- [39] Peterson D R and Hecht K T 1980 *Nucl. Phys. A* **344** 361
- [40] Rosensteel G and Rowe D J 1980 *Ann. Phys., NY* **126** 343
- [41] Draayer J P, Weeks K J and Rosensteel G 1984 *Nucl. Phys. A* **413** 215
- [42] Avancini S S and de Passos E J V 1993 *J. Phys. G: Nucl. Part. Phys.* **19** 125